

Impact of message fatigue and individual behavioral responses on epidemiological spread in temporal simplicial networks

Xiao-Nan Fan(樊晓楠) and Xuemei You(由雪梅)

Citation: Chin. Phys. B, 2025, 34 (**3**): 038703. DOI: 10.1088/1674-1056/adaade
Journal homepage: http://cpb.iphy.ac.cn; http://iopscience.iop.org/cpb

What follows is a list of articles you may be interested in

Reconstructing *in vivo* spatially offset Raman spectroscopy of human skin tissue using a GPU-accelerated Monte Carlo platform

Yun-He Zhang(张云鹤), Huan-Zheng Zhu(朱桓正), Yong-Jiang Dong(董泳江), Jia Zeng(曾佳), Xin-Peng Han(韩新鹏), Ivan A. Bratchenko, Fu-Rong Zhang(张富荣), Si-Yuan Xu(许思源), and Shuang Wang(王爽)
Chin. Phys. B, 2023, 32 (**11**): 118702. DOI: 10.1088/1674-1056/acef05

GEANT4 simulation study of over-response phenomenon of fiber x-ray sensor

Bin Zhang(张彬), Tian-Ci Xie(谢天赐), Zhuang Qin(秦壮), Hao-Peng Li(李昊鹏), Song Li(李松), Wen-Hui Zhao(赵文辉), Zi-Yin Chen(陈子印), Jun Xu(徐军), Elfed Lewis, and Wei-Min Sun(孙伟民)
Chin. Phys. B, 2021, 30 (**4**): 048701. DOI: 10.1088/1674-1056/abcfa6

Electron beam irradiation on novel coronavirus (COVID-19): A Monte-Carlo simulation

Guobao Feng(封国宝), Lu Liu(刘璐), Wanzhao Cui(崔万照), Fang Wang(王芳)
Chin. Phys. B, 2020, 29 (**4**): 048703. DOI: 10.1088/1674-1056/ab7dac

Phase transition of DNA compaction in confined space: Effects of macromolecular crowding are dominant

Erkun Chen(陈尔坤), Yangtao Fan(范洋涛), Guangju Zhao(赵光菊), Zongliang Mao(毛宗良), Haiping Zhou(周海平), Yanhui Liu(刘艳辉)
Chin. Phys. B, 2020, 29 (**1**): 018701. DOI: 10.1088/1674-1056/ab5941

Application of microdosimetry on biological physics for ionizing radiation

Dandan Chen(陈丹丹), Liang Sun(孙亮)
Chin. Phys. B, 2018, 27 (**2**): 028701. DOI: 10.1088/1674-1056/27/2/028701

SPECIAL TOPIC — Computational programs in complex systems

Impact of message fatigue and individual behavioral responses on epidemiological spread in temporal simplicial networks

Xiao-Nan Fan(樊晓楠) and Xuemei You(由雪梅)[†]

Business School, Shandong Normal University, Jinan 250014, *China*

(Received 26 November 2024; revised manuscript received 3 January 2025; accepted manuscript online 16 January 2025)

Health information spreads rapidly, which can effectively control epidemics. However, the swift dissemination of information also has potential negative impacts, which increasingly attracts attention. Message fatigue refers to the psychological response characterized by feelings of boredom and anxiety that occur after receiving an excessive amount of similar information. This phenomenon can alter individual behaviors related to epidemic prevention. Additionally, recent studies indicate that pairwise interactions alone are insufficient to describe complex social transmission processes, and higher-order structures representing group interactions are crucial. To address this, we develop a novel epidemic model that investigates the interactions between information, behavioral responses, and epidemics. Our model incorporates the impact of message fatigue on the entire transmission system. The information layer is modeled using a static simplicial network to capture group interactions, while the disease layer uses a time-varying network based on activity-driven model with attractiveness to represent the self-protection behaviors of susceptible individuals and self-isolation behaviors of infected individuals. We theoretically describe the co-evolution equations using the microscopic Markov chain approach (MMCA) and get the epidemic threshold. Experimental results show that while the negative impact of message fatigue on epidemic transmission is limited, it significantly weakens the group interactions depicted by higher-order structures. Individual behavioral responses strongly inhibit the epidemic. Our simulations using the Monte Carlo (MC) method demonstrate that greater intensity in these responses leads to clustering of susceptible individuals in the disease layer. Finally, we apply the proposed model to real networks to verify its reliability. In summary, our research results enhance the understanding of the information–epidemic coupling dynamics, and we expect to provide valuable guidance for managing future emerging epidemics.

Keywords: Monte Carlo simulation, microscopic Markov chain approach, message fatigue, information–epidemic coupled spreading, simplicial complex

PACS: 87.19.X–, 02.50.Ga, 02.70.Uu, 05.10.–a

DOI: 10.1088/1674-1056/adaade **CSTR:** 32038.14.CPB.adaade

1. Introduction

Throughout history, infectious diseases have persistently impacted human societies, posing significant threats to life and property.[1] Notable examples include the smallpox virus,[2] the Spanish flu,[3] and the recent corona virus disease 2019 (COVID-19) pandemic.[4] These public health crises have endangered lives and impeded socioeconomic development.[5] Consequently, understanding disease transmission patterns and their influencing factors is crucial to mitigating the damage caused by such emergencies. The transmission dynamics of epidemic represent a highly complex system, necessitating substantial computational efforts to investigate the mechanisms of transmission and the various influencing factors. Numerous studies have identified various factors affecting epidemic transmission, such as network topology,[6] specific infection schemes,[7,8] policy interventions,[9] and immunization strategies.[10]

Among these, the coupled spreading of information–epidemics has garnered substantial research interest both domestically and internationally. At first, Funk *et al.*[11] developed a mathematical model to explore the impact of information diffusion on disease transmission, revealing that disease-related information spreading can reduce disease incidence and sometimes prevent outbreaks entirely. A substantial body of research indicates that epidemic spreading and information diffusion are interconnected processes: information diffusion can curb the spread of epidemic, while epidemics can drive the dissemination of information. The multi-layer network framework provides a more comprehensive representation of cooperative transmission systems for both information and diseases. Consequently, Granell *et al.*[12] introduced the unaware–aware–unaware-susceptible–infected–susceptible (UAU-SIS) model based on multilayer network theory to discuss the coupling effect of information–epidemic coupling spreading, determining the epidemic outbreak threshold using the MMC method. Other researchers have also delved into the interaction between information diffusion and disease transmission from various angles, including network structure,[13] resource allocation,[14] vaccination,[15]

[†]Corresponding author. E-mail: youxuemei@sdnu.edu.cn

© 2025 Chinese Physical Society and IOP Publishing Ltd. All rights, including for text and data mining, AI training, and similar technologies, are reserved.

attitude tendencies,[16] and mass media.[17]

In previous research on complex networks, interactions between pairs of nodes have often been assumed to be fundamental to the connections between system units. However, a thorough explanation of many complex systems necessitates further refinement of network system structural modeling. Group interactions necessitate improved network system formulations.[18,19] Some researchers have demonstrated that higher-order structures, such as simplicial complexes, are effective frameworks for representing the organization of various social, biological, and other systems involving interactions among three or more components.[20] Iacopini *et al.*[21] initially proposed a complex simplicial model for social contagion to account for interactions among groups of different sizes. This model integrates both pairwise and group interactions, effectively combining the core elements of simple and complex contagion processes. The research conducted by the authors establishes a foundational basis for subsequent investigations into the propagation dynamics within higher-order networks. The process of epidemic transmission occurs through the physical contact network, where variations in contact frequency and contact preferences among individuals significantly influence the dynamics of spread. Therefore, Wang *et al.*,[22] within the framework of multilayer networks, described the synergistic reinforcement of group interactions through simplicial complex structures on the information layer and constructed a temporal network with memory effects in the disease layer. They found that the synergistic reinforcement of higher-order interactions helps to inhibit the epidemic spread. The spatial distribution of the population and the community structure of the network significantly influence the coupled spreading dynamics of information diseases. Zhang *et al.*[23] developed a two-layer metapopulation network model. The information layer considers individual self-awareness, neighboring awareness, and group awareness, while the lower layer handles the spatial dynamics of epidemic spread. Fan *et al.*,[24] based on the UAU-SIS model, specifically used a Gaussian-like threshold model to describe the information diffusion process. Their study found that threshold models based on random simplicial networks may still lead to abrupt changes in epidemic thresholds.

When an epidemic occurs, people adjust their behavior based on epidemic-related information to mitigate infection risk, and these individual behavioral changes significantly influence the spread of the epidemic. Recently, researchers have begun to focus on the relationship among information, behavior, and epidemics. Wu *et al.*[25] developed an information–behavior–epidemic coupling model to study how government policies influence the co-evolution of information diffusion, vaccination behavior, and epidemic spreading. Their findings show that when government policies effectively coordinate across these areas, infection rates are minimized, resulting in optimal disease control. Huo *et al.*[26] examined how individuals' self-awareness and physical fitness influence information–behavior–epidemic coupling dynamics within a multiplex network environment. They used the threshold model to analyze how the behavior adoption process affects spreading across layers and assumed that variations in recognition ability and physical fitness follow a Gaussian distribution. Nevertheless, the majority of these studies have primarily concentrated on the co-evolutionary dynamics of information dissemination and epidemic spread within static multilayer networks. In reality, both network structures and individual interactions are subject to temporal changes; the contact relationships among individuals are not fixed but rather fluctuate over time. Consequently, numerous researchers have commenced utilizing the temporal network framework within the disease layer to delineate alterations in the physical contact network. For example, Pozzana *et al.*[27] explored disease transmission in an activity-driven model with attractiveness and discovered that a negative correlation between activity and attractiveness could raise the outbreak threshold. Huo *et al.*[28] proposed a three-layer coupled model to analyze the dynamic process of official information diffusion, protective behavior adoption and epidemic spreading in multiplex networks, focusing on individual heterogeneity in behavior adoption patterns. Xu *et al.*[29] introduced a multilayer activity-driven network model with heterogeneous personal edge activation to examine the impact of varied behaviors. Xie *et al.*[30] considered power-law distributions to examine the impact of asymmetric activity levels on information–epidemic coupling system, revealing a mapping relationship among partial nodes within the network. Peng *et al.*[31] developed a highly integrated effective degree approach to modeling epidemic and awareness spreading processes on multiplex networks coupled with awareness-dependent adaptive rewiring. This approach keeps track of the number of nearest neighbors in each state of an individual. In the aforementioned studies, the evolution of the network and the propagation process are treated as independent phenomena. However, in real-world scenarios, individuals frequently modify their behavioral responses in reaction to the spread of epidemics. Consequently, it is essential to examine the interplay between the evolution of network structure and the dynamics of propagation in related research.

During the spread of an epidemic, individuals' accurate comprehension of disease-related information and heightened awareness of epidemic prevention can effectively decrease their risk of infection and halt further spread of the epidemic.[32,33] However, the adverse effects of information dissemination are frequently disregarded, and message fatigue has started to garner scholarly attention. Message fatigue is prevalent during the epidemic transmission phase; it is a psychological reaction to repetitive information, typically resulting in the avoidance of similar information. This societal

phenomenon undeniably influences individual behavior and, consequently, the progression of the epidemic. Koh *et al.*[34] were the first to identify that the dissemination of epidemic-related information during the COVID-19 outbreak could result in message fatigue. They suggested that individuals, due to exposure to alarming health news, may experience short-term anxiety, especially after repeated presentation of such information, leading to weariness. This phenomenon of message fatigue may cause individuals to adopt other unhealthy behaviors. The phenomenon of message fatigue significantly contributes to aversion towards social media, resulting in behaviors such as social media distancing and the avoidance of information.[35] Then, Guo *et al.*[36] examined how information irrelevance and overload contribute to social media fatigue and its link to information avoidance behavior. The study revealed that social media fatigue may mediate the relationship between information overload and avoidance behavior. Furthermore, the impact of message fatigue is not limited to the COVID-19. Walker *et al.*[37] investigated the acquired immune deficiency syndrome (AIDS) risk awareness among South African youth in 2020 and found that the extensive dissemination of AIDS-related content has led to increasing indifference to health information. Message fatigue can lead to extreme behaviors and emotional responses, resulting in a failure to correctly perceive the severity of the epidemic and affecting individual behavioral responses. In the era of information globalization, the phenomenon of message fatigue may be challenging to circumvent. This phenomenon places significant pressure on government and societal efforts to control epidemics. Thus, it is significant to consider message fatigue in dissemination dynamics models and examine its impact on the evolution of epidemic transmission.

Inspired by the aforementioned studies, we consider the factor of message fatigue and propose a new information–epidemic coupling model (UAF-SIS) based on a two-layer network framework to describe information–epidemic coupling spreading. Given that online social relationships among users are generally stable,[38] we construct a higher-order static network in the information layer using a 2-simplicial complex structure to represent the complex information dissemination process. Additionally, we account for the heterogeneity of individual behavioral changes by constructing a disease layer based on an activity-driven network model with attractiveness to represent the epidemic spread process. We then use the microscopic Markov chain approach (MMCA) to characterize information–epidemic coupling spreading and get the epidemic outbreak threshold. We also perform Monte Carlo (MC) simulations to model changes in network topology. Finally, we apply the proposed model to a typical real-world network and find that the results are consistent with those obtained from artificial networks, validating the reliability of our model. Our study yields the following findings.

(i) Self-protective and self-isolation behaviors adopted by individuals significantly suppress the spread of epidemics.

(ii) Self-protective behavior reduces the average degree of the disease layer network, increases the number of low-degree nodes, and decreases the proportion of high-degree nodes.

(iii) Self-protective and self-isolation behaviors lead to the clustering of susceptible nodes in the disease layer network.

(iv) Message fatigue can, to some extent, hinder the process of information dissemination, thus facilitating the spread of epidemics.

(v) Higher-order interactions of information dissemination can, to some extent, facilitate the information dissemination process, thereby inhibiting the spread of epidemics.

The paper is structured as follows: Section 2 details the dynamics and interaction mechanisms of the information–epidemic coupling transmission model on higher-order temporal networks. Section 3 uses the MMCA to analyze the model and derive an analytical expression for the epidemic threshold. Section 4 explores the impact of various parameters on epidemic spread through simulations on artificial networks, using the MC method to simulate changes in the disease layer network's topology. Section 5 applies our model to real-world networks to verify its reliability. Finally, Section 6 concludes the study.

2. UAF-SIS model description

We first construct a multi-layer network with two layers: the upper information layer and the lower disease layer. Both layers have the same set of nodes but different topological structures. The information layer is a 2-simplicial complex, where epidemic information spreads according to the unaware–aware–fatigue (UAF) process, considering group interactions. Meanwhile, the physical contact layer is modeled as a time-varying network built using an attractive active-driven model and features a susceptible–infectious–susceptible (SIS) model. Figure 1 illustrates a simple schematic of the UAF-SIS model. For simplicity, we assume that both two-layer networks are undirected and unweighted, with a one-to-one correspondence between their nodes. The model details are described as follows.

First, the information layer network is generated using a random simplicial complex algorithm, producing 2-dimensional simplicial complexes. The process involves the following steps: (i) Start with N nodes. Connect any two nodes $i, j \in V$ with a probability $p_| \in [0,1]$, resulting in an average degree of $(N-1)p_|$. (ii) For any $i, j, k \in V$, add a 2-simplex (i, j, k) with a probability $p_\Delta \in [0,1]$. At this stage, each node has an average of $\langle k_\Delta \rangle = (N-1)(N-2)p_\Delta/2$ 2-simplices, which contributes to the node's degree. This method allows for generating simplicial complexes with the desired average

degrees $\langle k_| \rangle$ and $\langle k_\Delta \rangle$.

$$\begin{cases} p_| = \dfrac{\langle k_| \rangle - 2\langle k_\Delta \rangle}{(N-1) - 2\langle k_\Delta \rangle}, \\ p_\Delta = \dfrac{2\langle k_\Delta \rangle}{(N-1)(N-2)}. \end{cases} \tag{1}$$

According to the literature,[36] message fatigue anxiety triggered by alarming health news can lead to fatigue after repeated exposure to such information. In epidemic research, message fatigue can lead to individuals becoming less responsive or even resistant to epidemic-related information, which can affect their epidemic prevention behaviors. In the proposed model, it is assumed that individuals in the aware state might experience fatigue. This means that when individuals experience excessive exposure to epidemic information, leading to reduced sensitivity to the information, message fatigue may occur. Message fatigue can make people react negatively to epidemic prevention measures, affecting their ability to engage in effective preventive behaviors.

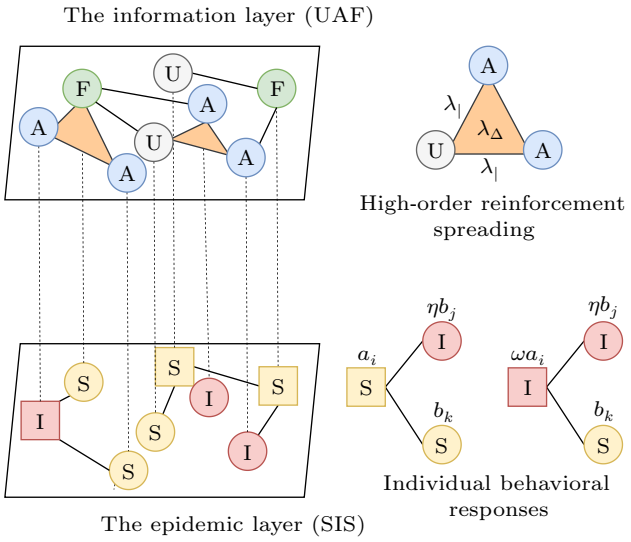


Fig. 1. Schematic of the coupled UAF-SIS model. The upper layer is a static simplicial network, with nodes in three states: gray for unaware (U), light blue for aware (A), and green for fatigue (F). The lower layer is a temporal network using an active-driven model with attractiveness, with nodes in two states: yellow for susceptible (S) and red for infected (I). Circles represent inactive nodes, and squares represent active nodes. The parameter m is set to 2.

Therefore, nodes can be categorized into three states in the upper information layer: (i) unaware (U); (ii) aware (A); (iii) fatigued (F). The information diffusion process is as follows: Nodes in the A state are aware of information about epidemic, and they can diffuse disease-related information to their neighbors and take preventive measures to prevent being infected. The nodes in the U state are unaware of the epidemic-related information, do not disseminate it, and do not adopt any protective measures. Nodes in the F state are individuals who have become fatigued by the epidemic information; they no longer spread disease-related information but will still take appropriate preventive behavior. The UAF state transition diagram is shown in Fig. 1. In the UAF model, nodes in the U state can transition to the A state through three mechanisms: First, if a node is infected, it automatically moves to the A state. Second, a node i can become aware by interacting with an A state neighbor with probability $\lambda_|$, representing edge transmission. Third, due to synergistic reinforcement, if both of the other nodes in a 2-simplex are in the A state, node i will be informed with probability λ_Δ, representing higher-order transmission.

Additionally, individuals in the A and F states may forget epidemic-related information with probabilities σ_A and σ_F, respectively. Moreover, considering that in the real world, people are more likely to experience message fatigue when the threat of the epidemic is low, and are less likely to become fatigued when the threat is high, our model reflects this by incorporating the following behavior: the aware node may transition to the fatigue node with probability $\tau(t)$. To account for the impact of the disease's scale on the transition of A individuals to the F state, we design the following formula:

$$\tau(t) = \pi^{\rho^{\mathrm{I}}(t)}. \tag{2}$$

Here, $\pi \in [0,1]$ is defined as the modulation factor that regulates the transition of all aware (A state) nodes to fatigued (F state) nodes. This means that when the epidemic is not active, $\rho^{\mathrm{I}}(t)$, and $\tau(t) = 1$, which indicates that over time, individuals may perceive the epidemic as posing no threat and quickly become fatigued with the epidemic-related information. Specifically, we assume that individuals infected with the disease will not forget the epidemic-related information before they recover.

In real world, many temporal interactions cannot be explained and encoded through local action mechanisms. For example, in social networks, people often interact with influential users with higher probabilities, reflecting their impact and popularity. This behavior results from global influences rather than local mechanisms. Therefore, we introduce an attractiveness feature b_i for each node, which affects the way that active nodes choose their interaction partners through global effects.

Our disease layer network is generated using an activity-driven network model with attractiveness.[39] The essence of the activity-driven model with attractiveness is to assign each node two attributes: activity a_i and attractiveness b_i. The activity level a_i represents the probability that node i will activate and form new interactions at each time step, reflecting its tendency to interact. Conversely, the attractiveness level b_i indicates the probability that node i will attract active nodes to connect with it at each time step. Additionally, during an epidemic, infected individuals reduce their activity and attractiveness by isolating themselves and taking protective measures. Therefore, we introduce parameters ω and η to represent the

factors that adjust the activity and attractiveness of infected individuals, respectively. These parameters correspond to self-protection behaviors such as maintaining safe social distances and self-isolation. The introduction of the behavior change mechanism into the attractive active-driven model can be described as follows:

Step 1 Given the joint probability distribution $H(f,g) \propto f^{-\gamma_a} g^{-\gamma_b}$, $(\varepsilon \le f_i \le 1, \varepsilon \le g_i \le 1)$, assign the activity potential f_i and attractiveness potential g_i to each node i. Each node's activity level and attractiveness are represented by $a_i = \zeta f_i$ and $b_i = \zeta g_i$, respectively.

Step 2 At each discrete time step t, a node i in state $X \in \{\mathrm{S},\mathrm{I}\}$ becomes active with probability $a_{i,X}\Delta t$ and creates m edges with other nodes in the network G_t. Active nodes connect to target nodes based on their attractiveness $b_{j,X}\Delta t$, with the probability of choosing one node being proportional to its attractiveness.

Step 3 Epidemic dynamics occur on the network G_t.

Step 4 At the next time step $t+\Delta t$, all edges in the network G_t are removed, and the process returns to Step 2.

We utilize the classical SIS epidemic model to depict the epidemic spreading in the lower disease layer. For a susceptible node, its infection rate in the disease layer depends on its state X in the upper information layer. Specifically, if a node is in state $X \in \{\mathrm{U},\mathrm{A},\mathrm{F}\}$, the infection rate is $\beta^X = \beta\theta_X(t)$. Moreover, an infected state node can recover with a probability of μ. Without effective treatments and with limited medical resources, individuals may increasingly depend on the information they receive to guide their behaviors and prevent infection. While existing models often assume constant behavioral responses, the reality is more complex, as individual behaviors can shift with changing information. Therefore, it is crucial to examine the interplay between information and behavioral responses. We connect protective behaviors to the scale of information diffusion and define $\theta_X(t)$ as follows:

$$\theta_X(t) = 1-(1-\sigma_X)^{\rho^{\mathrm{A}}(t)}, \quad X \in \{\mathrm{U},\mathrm{A},\mathrm{F}\}, \tag{3}$$

where $\sigma_X \in (0,1]$ represents the strength of the behavioral response, indicating how effectively the information influences behavior. $\theta_X(t)$ is proportional to the global amount of awareness $\rho^{\mathrm{A}}(t)$. When no information is available $\rho^{\mathrm{A}}(t)=0$, $\theta_X(t)=0$, meaning individuals do not engage in protective behavior, and the infection rates remain $\beta^{\mathrm{U}} = \beta^{\mathrm{A}} = \beta^{\mathrm{F}} = \beta$. When information is fully diffused $\rho^{\mathrm{A}}(t)=1$, individuals will engage in protective behavior with probability σ_X.

3. Analytical results based on MMCA

The microscopic Markov chain is a specific type of Markov chain model utilized to characterize the behavior and state transitions of individuals or particles within complex systems. At the microscopic level, individuals or particles can occupy various states, and these states may evolve over time. The microscopic Markov chain delineates the transitions between these states by establishing the state space and the associated state transition probabilities. In our model, $r_i^{\downarrow}(t)$ represents that node i does not received disease-related information by its pairwise neighbors Γ_i. $r_i^{\Delta}(t)$ means that node i does not received disease-related information by its 2-simplicial neighbors Δ_i. The probabilities $q_i^{\mathrm{U}}(t)$, $q_i^{\mathrm{A}}(t)$ and $q_i^{\mathrm{F}}(t)$ respectively represent the likelihood that susceptible node i in unaware (U), aware (A), or fatigued (F) state is not infected by its neighbors. Thus, based on the proposed UAF-SIS model description, the formulas are as follows:

$$\begin{cases} r_i^{\downarrow}(t) = \prod\limits_{j\in\Gamma_i}\left[1-\lambda_{\downarrow}P_j^{\mathrm{A}}(t)\right], \\ r_i^{\Delta}(t) = \prod\limits_{j,k\in\Delta_i}\left[1-\lambda_{\Delta}P_j^{\mathrm{A}}(t)P_k^{\mathrm{A}}(t)\right], \\ r_i(t) = r_i^{\downarrow}(t)r_i^{\Delta}(t), \\ q_i^{\mathrm{U}}(t) = \prod\limits_j\left\{1-\beta\dfrac{m}{N}\left[\eta a_i b_j P_j^{\mathrm{I}}(t)+\omega a_j b_i P_j^{\mathrm{I}}(t)\right]\right\}, \\ q_i^{\mathrm{A}}(t) = \prod\limits_j\left\{1-\beta\left[1-\theta_{\mathrm{A}}(t)\right]\dfrac{m}{N}\right. \\ \qquad\qquad \left.\times\left[\eta a_i b_j P_j^{\mathrm{I}}(t)+\omega a_j b_i P_j^{\mathrm{I}}(t)\right]\right\}, \\ q_i^{\mathrm{F}}(t) = \prod\limits_j\left\{1-\beta\left[1-\theta_{\mathrm{F}}(t)\right]\dfrac{m}{N}\right. \\ \qquad\qquad \left.\times\left[\eta a_i b_j P_j^{\mathrm{I}}(t)+\omega a_j b_i P_j^{\mathrm{I}}(t)\right]\right\}. \end{cases} \tag{4}$$

Based on the state transition tree in Fig. 2, we can derive the following UAF-SIS state evolution equations using the MMCA method:

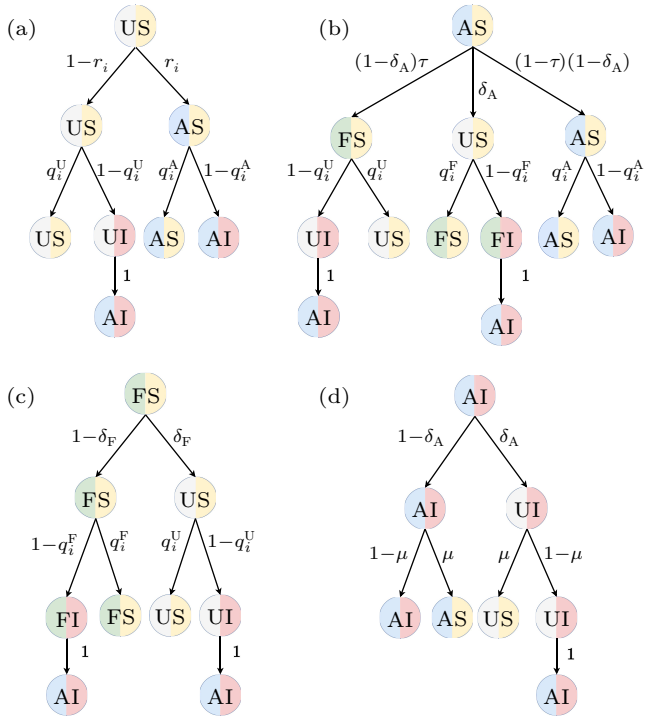


Fig. 2. State transition tree of the UAF-SIS model.

$$
\begin{cases}
P_i^{\mathrm{US}}(t+1) = P_i^{\mathrm{US}}(t) r_i(t) q_i^{\mathrm{U}}(t) + P_i^{\mathrm{AS}}(t)\delta_{\mathrm{A}} q_i^{\mathrm{U}}(t) \\
\qquad + P_i^{\mathrm{FS}}(t)\delta_{\mathrm{F}} q_i^{\mathrm{U}}(t) + P_i^{\mathrm{AI}}(t)\delta_{\mathrm{A}}\mu, \\
P_i^{\mathrm{AS}}(t+1) = P_i^{\mathrm{US}}(t)\left[1-r_i(t)\right] q_i^{\mathrm{A}}(t) + P_i^{\mathrm{AS}}(t)(1-\delta_{\mathrm{A}}) \\
\qquad \times \left[1-\tau(t)\right] q_i^{\mathrm{A}}(t) + P_i^{\mathrm{AI}}(t)(1-\delta_{\mathrm{A}})\mu, \\
P_i^{\mathrm{FS}}(t+1) = P_i^{\mathrm{AS}}(t)(1-\delta_{\mathrm{A}})\tau(t) q_i^{\mathrm{F}}(t) \\
\qquad + P_i^{\mathrm{FS}}(t)(1-\delta_{\mathrm{F}}) q_i^{\mathrm{F}}(t) \\
\qquad + P_i^{\mathrm{AI}}(t)(1-\delta_{\mathrm{A}})\tau(t)\mu, \\
P_i^{\mathrm{AI}}(t+1) = P_i^{\mathrm{US}}(t) r_i(t)\left[1-q_i^{\mathrm{U}}(t)\right] \\
\qquad + P_i^{\mathrm{US}}(t)\left[1-r_i(t)\right]\left[1-q_i^{\mathrm{A}}(t)\right] \\
\qquad + P_i^{\mathrm{AS}}(t)\delta_{\mathrm{A}}\left[1-q_i^{\mathrm{U}}(t)\right] \\
\qquad + P_i^{\mathrm{AS}}(t)\left[1-\delta_{\mathrm{A}}\right]\left[1-\tau(t)\right]\left[1-q_i^{\mathrm{A}}(t)\right] \\
\qquad + P_i^{\mathrm{AS}}(t)\left[1-\delta_{\mathrm{A}}\right]\tau(t)\left[1-q_i^{\mathrm{F}}(t)\right] \\
\qquad + P_i^{\mathrm{FS}}(t)\delta_{\mathrm{F}}\left[1-q_i^{\mathrm{U}}(t)\right] \\
\qquad + P_i^{\mathrm{FS}}(t)\left[1-\delta_{\mathrm{F}}\right]\left[1-q_i^{\mathrm{F}}(t)\right] + P_i^{\mathrm{AI}}(t)(1-\mu),
\end{cases}
\tag{5}
$$

when $t \to \infty$, the system reaches a steady state, at which point we can obtain

$$
\begin{cases}
P_i^{\mathrm{US}}(t+1) = P_i^{\mathrm{US}}(t) = P_i^{\mathrm{US}}, \\
P_i^{\mathrm{AS}}(t+1) = P_i^{\mathrm{AS}}(t) = P_i^{\mathrm{AS}}, \\
P_i^{\mathrm{FS}}(t+1) = P_i^{\mathrm{FS}}(t) = P_i^{\mathrm{FS}}, \\
P_i^{\mathrm{AI}}(t+1) = P_i^{\mathrm{AI}}(t) = P_i^{\mathrm{AI}},
\end{cases}
\tag{6}
$$

when β approaches the outbreak threshold, the probability of a node being infected approaches 0. Thus, we can assume $P_i^{\mathrm{I}} = \varepsilon_i \ll 1$, and $\varepsilon_i > 0$. Additionally, $P_i^{\mathrm{A}} = P_i^{\mathrm{AS}} + P_i^{\mathrm{AI}} \approx P_i^{\mathrm{AS}}$P, and neglecting higher-order terms $O(\varepsilon_i)$, we simplify Eq. (5) to

$$
\begin{cases}
P_i^{\mathrm{U}} = P_i^{\mathrm{U}} r_i + P_i^{\mathrm{A}}\delta_{\mathrm{A}} + P_i^{\mathrm{F}}\delta_{\mathrm{F}}, \\
P_i^{\mathrm{A}} = P_i^{\mathrm{U}}(1-r_i) + P_i^{\mathrm{A}}(1-\delta_{\mathrm{A}})(1-\alpha_i), \\
P_i^{\mathrm{F}} = P_i^{\mathrm{F}}(1-\delta_{\mathrm{F}}) + P_i^{\mathrm{A}}(1-\delta_{\mathrm{A}})\alpha_i,
\end{cases}
$$

$$
\begin{aligned}
\varepsilon_i &= \varepsilon_i(1-\mu) + P_i^{\mathrm{U}}(1-q_i^{\mathrm{U}}) + P_i^{\mathrm{A}}(1-q_i^{\mathrm{A}}) + P_i^{\mathrm{F}}(1-q_i^{\mathrm{F}}) \\
&\approx m\beta(\eta a_i\varphi_b + \omega b_i\varphi_a)\left[1-\theta_{\mathrm{A}}P_i^{\mathrm{A}} - \theta_{\mathrm{F}}P_i^{\mathrm{F}}\right] \\
&= m\beta\Big\{\eta\left[a_i - (1-\theta_{\mathrm{A}}P_i^{\mathrm{A}} - \theta_{\mathrm{F}}P_i^{\mathrm{F}})\right]\varphi_b \\
&\quad + \omega\left[b_i - (1-\theta_{\mathrm{A}}P_i^{\mathrm{A}} - \theta_{\mathrm{F}}P_i^{\mathrm{F}})\right]\varphi_a\Big\},
\end{aligned}
\tag{7}
$$

where $\Phi_a = \frac{1}{N}\sum_{j=1}^{N} a_j\varepsilon_i$ and $\Phi_b = \frac{1}{N}\sum_{j=1}^{N} b_j\varepsilon_i$. Then, by averaging over all nodes, equation (7) can be further simplified to

$$
\begin{aligned}
\mu\varepsilon_i \;=\; & m\beta\Big\{\eta\left[\langle a\rangle - (1-\theta_{\mathrm{A}}P_i^{\mathrm{A}} - \theta_{\mathrm{F}}P_i^{\mathrm{F}})\right]\Phi_b \\
& + \omega\left[\langle b\rangle - (1-\theta_{\mathrm{A}}P_i^{\mathrm{A}} - \theta_{\mathrm{F}}P_i^{\mathrm{F}})\right]\Phi_a\Big\}.
\end{aligned}
\tag{8}
$$

By multiplying both sides of Eq. (8) by a_i and taking the average, we can obtain

$$
\begin{aligned}
\mu\varepsilon_i \;=\; & m\beta\Big\{\eta\left[\langle a^2\rangle - (1-\theta_{\mathrm{A}}P_i^{\mathrm{A}} - \theta_{\mathrm{F}}P_i^{\mathrm{F}})\langle a\rangle\right]\varphi_b \\
& + \omega\left[\langle ab\rangle - (1-\theta_{\mathrm{A}}P_i^{\mathrm{A}} - \theta_{\mathrm{F}}P_i^{\mathrm{F}})\langle a\rangle\right]\varphi_a\Big\}.
\end{aligned}
\tag{9}
$$

By multiplying both sides of Eq. (8) by b_i and taking the average, we can obtain

$$
\begin{aligned}
\mu\varepsilon_i \;=\; & m\beta\Big\{\eta\left[\langle ab\rangle - (1-\theta_{\mathrm{A}}P_i^{\mathrm{A}} - \theta_{\mathrm{F}}P_i^{\mathrm{F}})\langle b\rangle\right]\varphi_b \\
& + \omega\left[\langle b^2\rangle - (1-\theta_{\mathrm{A}}P_i^{\mathrm{A}} - \theta_{\mathrm{F}}P_i^{\mathrm{F}})\langle b\rangle\right]\varphi_a\Big\}.
\end{aligned}
\tag{10}
$$

Therefore, we can express Eqs. (8)–(10) in matrix form as

$$
H\begin{bmatrix}\varepsilon_i \\ \varphi_a \\ \varphi_b\end{bmatrix} = \frac{\mu}{m\beta}\begin{bmatrix}\varepsilon_i \\ \varphi_a \\ \varphi_b\end{bmatrix},
\tag{11}
$$

where

$$
H = \begin{bmatrix}
0 & \omega\left[\langle b\rangle - (1-\theta_{\mathrm{A}}P_i^{\mathrm{A}} - \theta_{\mathrm{F}}P_i^{\mathrm{F}})\right] & \eta\left[\langle a\rangle - (1-\theta_{\mathrm{A}}P_i^{\mathrm{A}} - \theta_{\mathrm{F}}P_i^{\mathrm{F}})\right] \\
0 & \omega\left[\langle ab\rangle - (1-\theta_{\mathrm{A}}P_i^{\mathrm{A}} - \theta_{\mathrm{F}}P_i^{\mathrm{F}})\langle a\rangle\right] & \eta\left[\langle a^2\rangle - (1-\theta_{\mathrm{A}}P_i^{\mathrm{A}} - \theta_{\mathrm{F}}P_i^{\mathrm{F}})\langle a\rangle\right] \\
0 & \omega\left[\langle b^2\rangle - (1-\theta_{\mathrm{A}}P_i^{\mathrm{A}} - \theta_{\mathrm{F}}P_i^{\mathrm{F}})\langle b\rangle\right] & \eta\left[\langle ab\rangle - (1-\theta_{\mathrm{A}}P_i^{\mathrm{A}} - \theta_{\mathrm{F}}P_i^{\mathrm{F}})\langle b\rangle\right]
\end{bmatrix},
\tag{12}
$$

when the network system reaches equilibrium, we have

$$
\begin{bmatrix}\varepsilon_i \\ \varphi_a \\ \varphi_b\end{bmatrix} \neq \mathbf{0},
\tag{13}
$$

when an epidemic breaks out in the network system, the epidemic threshold can be determined as the value of β_{C} that satisfies Eq. (11), such that $\mu/(m\beta)$ equals $\Lambda_{\max}(H)$, where $\Lambda_{\max}(H)$ is the largest eigenvalue of matrix H

$$
\beta_{\mathrm{C}} = \frac{\mu}{m\Lambda_{\max}(H)}.
\tag{14}
$$

Therefore, from Eq. (14), we can conclude that the threshold is affected by μ, the density of aware nodes ρ^{A} and fatigued nodes ρ^{F}. Meanwhile, the network structures of the information and disease layers are also very close to the epidemic threshold according to Eq. (14).

4. Application on artificial networks

In this section, we apply the UAF-SIS model to artificial networks to examine how different parameters affect the

spread dynamics. The network consists of $N = 500$ nodes, with an initial infection ratio $\rho^{\mathrm{AI}}(0) = 0.1$. In the iterative calculations of the micro-Markov chain, the infected nodes can be represented as $\rho^{\mathrm{AI}}(t) = 1/N\sum_i \rho_i^{\mathrm{AI}}(t)$. In the information layer, we apply the random simplicial complex algorithm to construct a second-order simplicial complex network. The disease layer is created using an activity-driven model with attractiveness. In the subsequent experiments, the default parameter values are set as follows: $\gamma_a = \gamma_b = \gamma$, $\zeta = 4$, $\langle k_| \rangle = 8$, $\langle k_\Delta \rangle = 3$, $\mu = 0.2$, $\sigma_{\mathrm{A}} = \sigma\sigma_{\mathrm{F}} = \sigma^2 = 0.25$, $\delta_{\mathrm{A}} = \delta_{\mathrm{F}} = 0.6$.

In Fig. 3, we illustrate a comparative experiment of the information diffusion and epidemic spreading processes between the UAF-SIS and the UAU-SIS model. In Fig. 3, the blue and orange lines illustrate the information propagation scale of the classical model and the proposed model, respectively. It is evident that the proposed model accounts for the influence of message fatigue, resulting in a significant number of conscious individuals becoming fatigued. Consequently, the proportion of conscious individuals within the system is greatly diminished. The green and red lines represent the scale of epidemic spreading in both models. Individual actions taken in response to epidemic spreading lead to a substantial reduction in the scale of epidemic spreading and an increase in the outbreak threshold. Therefore, taking into account the message fatigue factor and individual behavioral responses can help mitigate the scale of information–epidemic spreading.

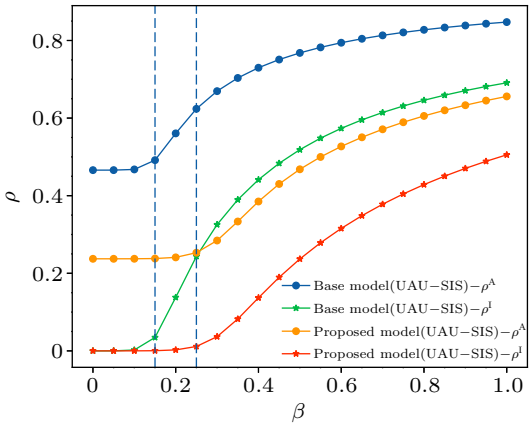


Fig. 3. Comparison of information–epidemic coupled spread in UAU-SIS model and UAF-SIS model. The blue dashed line represents the epidemic outbreak threshold. The parameters are set as follows: $\lambda_| = 0.2$, $\lambda_\Delta = 0.3$, $\omega = 0.8$, $\eta = 0.6$, $m = 4$.

First, we illustrate in Fig. 4 the impact of the self-protection factor ω and self-isolation factor η on the final scale of epidemic spread. The smaller the values of ω and η, the more pronounced the behavioral changes in infected nodes. As ω and η increase, the final infection size of the epidemic grows. A smaller ω implies that infected nodes are less likely to become active nodes during network construction and are less likely to establish connections with other individuals, mirroring the real scenario where infected nodes actively maintain safe social distances. A smaller η indicates that infected nodes encounter more difficulty in establishing connections with active susceptible nodes, reflecting the measures taken by infected nodes to self-isolate and prevent further epidemic spreading.

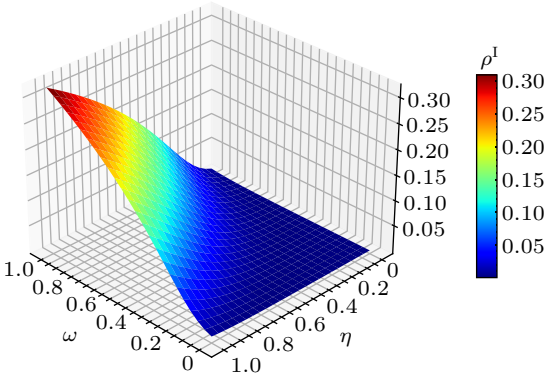


Fig. 4. Effects of self-protection factor ω and self-isolation factor η on the final infection size at steady state.

Next, we use the Monte Carlo (MC) numerical simulation method to simulate the network changes during the information–epidemic coupling spreading. MC numerical simulation method, often referred to as the statistical simulation method, is a stochastic simulation technique grounded in probability and statistical theory. This method employs random numbers, or more frequently, pseudo-random numbers, to address a variety of computational challenges.

We illustrate the impact of the self-protection factor ω and self-isolation factor η on the average degree $\langle k \rangle$ of the lower disease layer network in Fig. 5. Infection results in a decrease in an individual's activity and attractiveness, significantly influencing the network's structural characteristics. As depicted in Fig. 5(a), the decrease in the self-isolation factor ω has a minor effect on the network's average degree $\langle k \rangle$ when β is samll, as individuals do not change their behavior without infections. However, with an increase in β, the decline in the disease layer network's average degree $\langle k \rangle$ due to the self-protection factor η becomes more noticeable. The rise in infections leads to a decrease in the system's average activity, reducing active nodes and consequently lowering the network's average degree $\langle k \rangle$. The higher the infection rate, the more pronounced the suppressive effect of the self-protection factor ω on the average degree. In Fig. 5(b), the increase in the self-isolation factor η does not impact the network's average degree $\langle k \rangle$. The alteration in the average degree solely relies on the average activity level and the contact capability of active nodes, aligning with the findings in Ref. [27].

We will explore the impact of ω and η on the network edges in Fig. 6. When β is small, the impacts of ω and η on network edges are minimal because, in the absence of infected individuals, individuals do not alter their behavior. However, as β increases, the number of infected individuals in the network rises. Two behaviors can lead to a decrease in the average activity level and average attractiveness level in spreading sys-

tem, causing active susceptible nodes to be more likely to interact with other susceptible individuals, increasing the edges between susceptible nodes and resulting in clustering of susceptible nodes. Additionally, as the infection rate β increases, the impact of ω and η on the disease layer network edges becomes more pronounced.

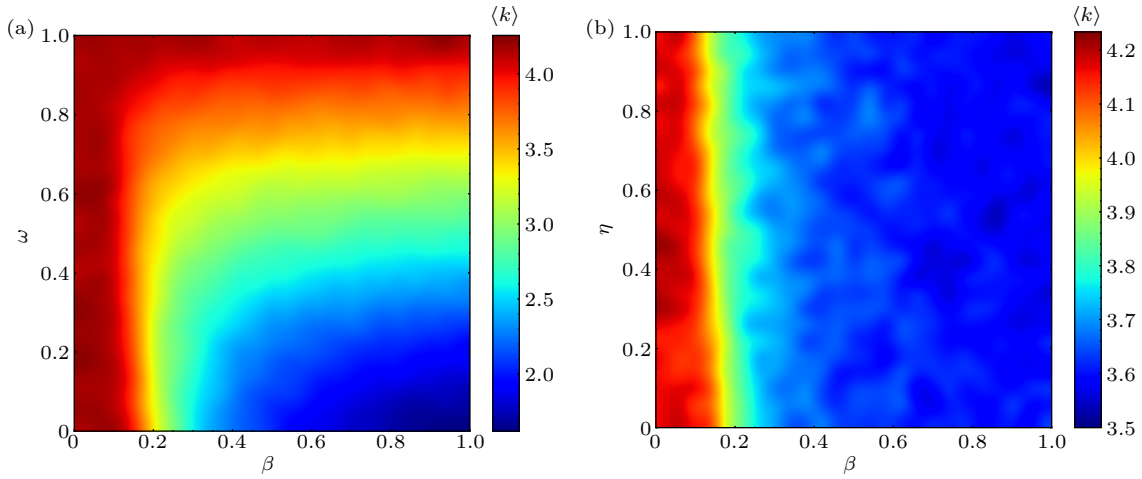


Fig. 5. The effects of (a) the self-protection factor ω and (b) self-isolation factor η on the average degree $\langle k \rangle$ of the disease layer network at steady state.

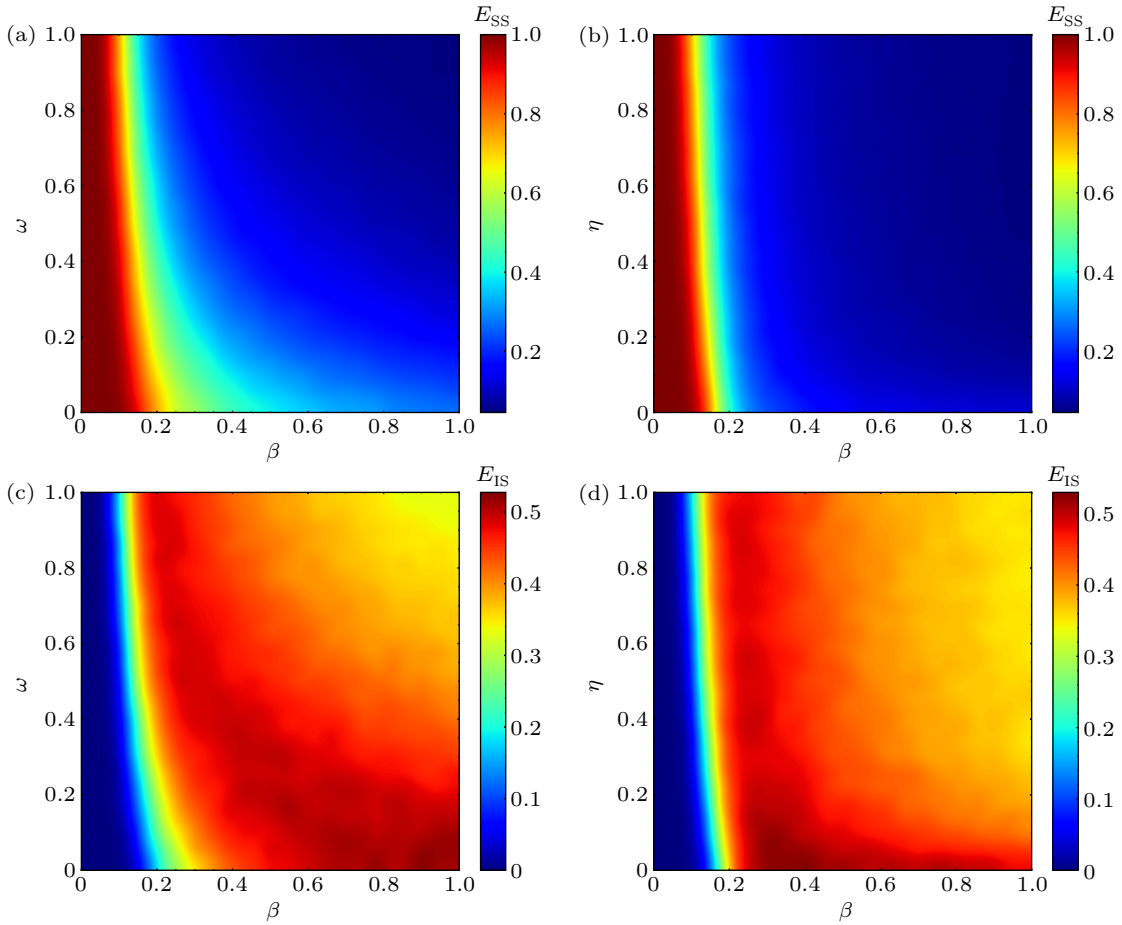


Fig. 6. The effects of (a), (c) the self-protection factor ω and (b), (d) self-isolation factor η on the edges of the disease layer network at steady state.

Additionally, in Fig. 7, we discuss the impact of ω and η on the evolution of the cumulative degree distribution in the temporal disease layer network. We examine the effects of ω and η by comparing the cumulative degree distribution of the network at the initial time with that at the final time. When ω and η are small, the response behavior of infected individuals is relatively strong in the comparison between Figs. 7(a) and 7(i). At equilibrium, the network has more small-degree nodes and fewer large-degree nodes, resulting in a decrease in the overall average degree of the network, which is consistent with the conclusion of Fig. 5(a). In Figs. 7(a)–7(c), with a fixed self-protection factor ω, as the self-isolation factor η in-

creases, the cumulative degree distribution of the disease layer network changes only slightly. However, in Figs. 7(a), 7(d), and 7(g), with a fixed η, as ω increases, the cumulative degree distributions of the network at the initial time and the final time become increasingly similar. Therefore, the self-protection factor ω significantly influences the evolution of the network's cumulative degree distribution, whereas the self-isolation factor η has a smaller impact.

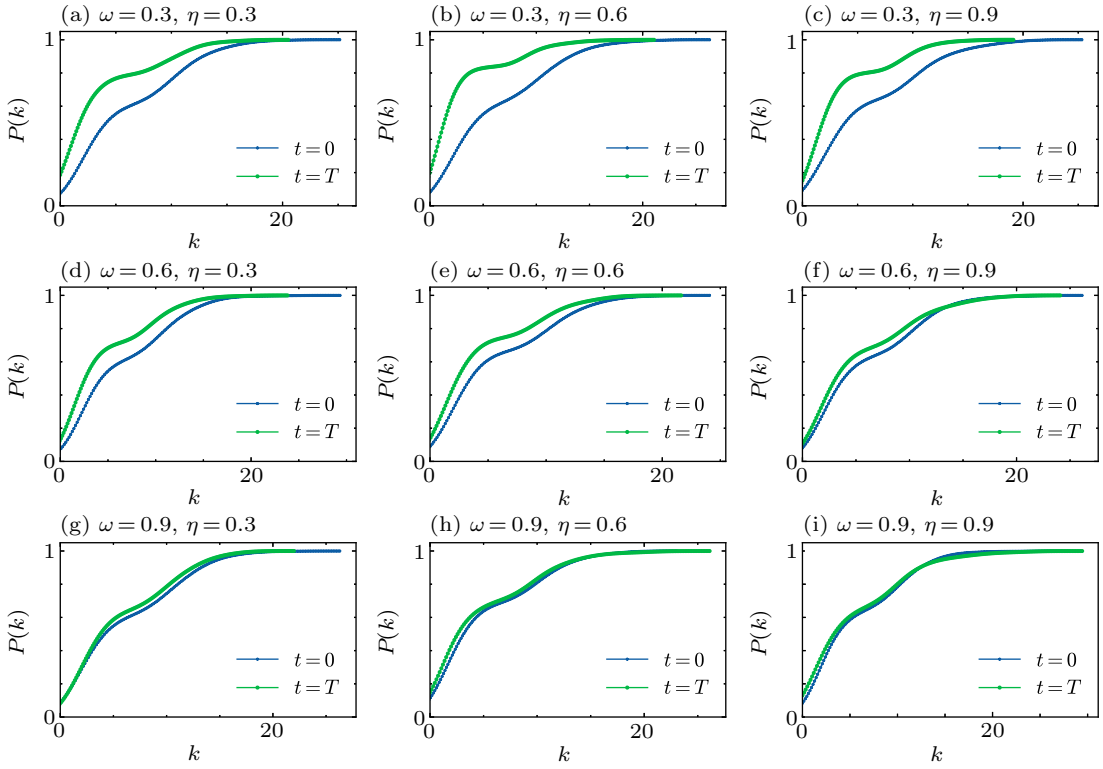


Fig. 7. The impact of the self-protection factor ω and self-isolation factor η on the degree distribution of the time-varying disease layer network.

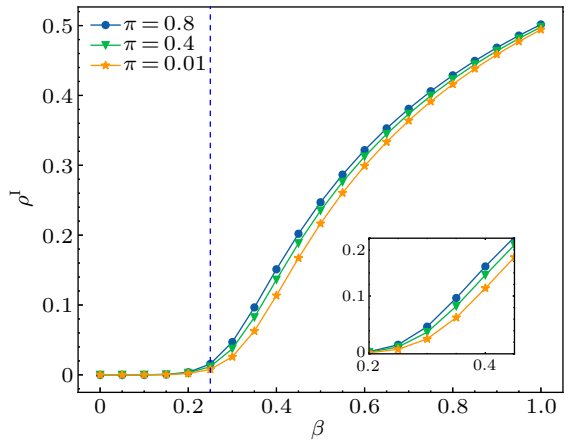


Fig. 8. The impact of message fatigue factor π on the final infection size at steady state.

Next, we discuss the impact of message fatigue on disease spreading in Fig. 8. The dashed blue line represents the threshold for an epidemic outbreak. In the inset, we have enlarged the curve depicting the changes in the final epidemic size for β ranging from 0.2 to 0.4 to emphasize the impact of the information fatigue factor π. As the message fatigue factor increases, the steady-state magnitude of the epidemic spread expands. This is due to a higher message fatigue factor π accelerating the rate at which conscious nodes are fatigued by the information, diminishing their response intensity and consequently heightening the risk of individual infection. Moreover, taking into account the effect of epidemic scale on message fatigue, when β is samll, the influence of message fatigue on the epidemic becomes more pronounced. At this juncture, the epidemic scale is smaller, and individuals are more susceptible to experiencing fatigue from health information. Conversely, when β is large and the epidemic spreading reaches a larger scale, individuals in such a perilous scenario do not encounter fatigue from health information, resulting in a minimal impact of message fatigue under high infection rates.

In Fig. 9, we examine the effects of information spread rate $\lambda_{|}$, λ_{Δ}, with β on the final infection size ρ^{I}. Clearly, when $\lambda_{|}$ and λ_{Δ} are fixed, the final infection size ρ^{I} increases with β. Additionally, increases in both the information spread rate $\lambda_{|}$ and λ_{Δ} lead to a decrease in the final infection size ρ^{I} , though high-order information spread rates λ_{Δ} have much less impact on the final infection size ρ^{I} compared to lower-order rates. For example, when $\beta=0.5$ and $\lambda_{|}=[0.25,0.5,0.75]$, the final infection size $\rho^{\mathrm{I}}=[0.0818,0.0705,0.0668]$ in Fig. 9(a). However, when both $\beta=0.5$ and $\lambda_{\Delta}=[0.25,0.5,0.75]$, the final infection size $\rho^{\mathrm{I}}=[0.1038,0.1008,0.0962]$ in Fig. 9(b). Clearly, the epidemic's spread size increases with β and decreases with increases in $\lambda_{|}$ and λ_{Δ}. Thus, enhancing the disease-related information spreading can, to some extent, help suppress the

epidemic spreading.

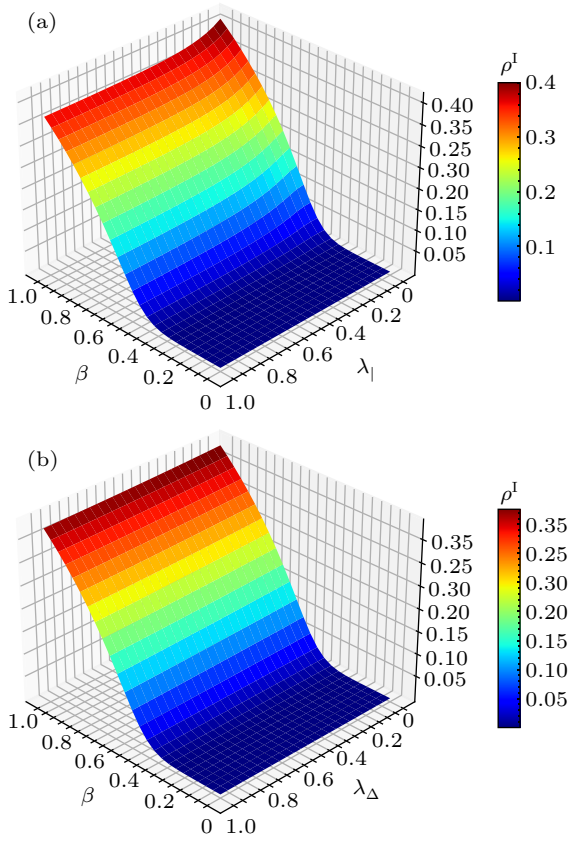


Fig. 9. Final infection scale at steady state with variations in information transmission rate $\lambda_{|}$, λ_{Δ} and infection rate β.

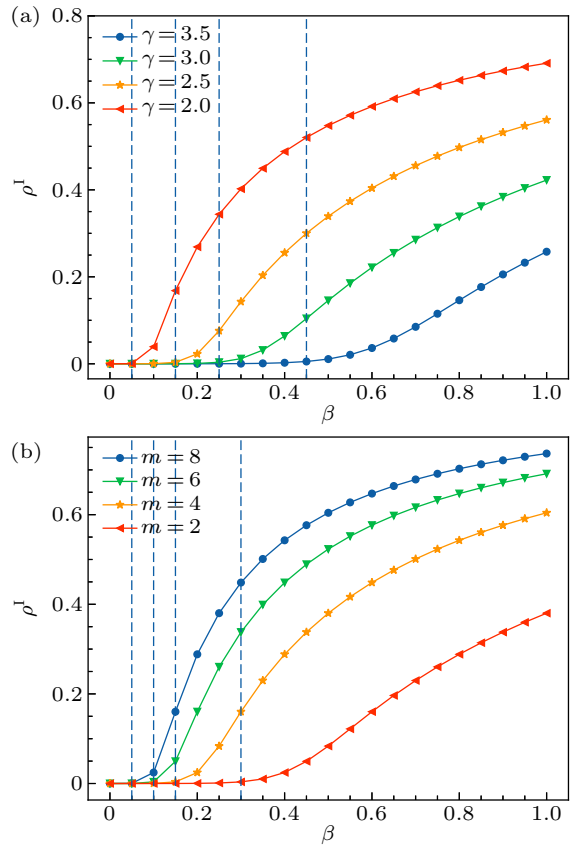


Fig. 10. The effects of node activity heterogeneity γ and the contact ability of active nodes m on the final infection size at steady state.

Finally, we examine the impact of node activity heterogeneity γ and the contact ability of active nodes m on the final infection size of the epidemic, as shown in Fig. 10. In Fig. 10(a), as the node activity heterogeneity γ increases, the final infection size decreases. This is because lower node activity heterogeneity implies the presence of highly active and attractive nodes in the disease layer network, which frequently establish connections and facilitate epidemic spread. Therefore, increasing node activity heterogeneity effectively inhibits the epidemic spreading. In Fig. 10(b), as the contact ability of active nodes m increases, the final infection size expands. Clearly, an increase in node contact ability results in more edges, increasing the probability of infected individuals connecting with susceptible nodes and thereby expanding the scale of epidemic spread.

5. Application on real networks

In this section, we apply the proposed framework to real-world networks to validate its applicability. Simulating the coevolution of disease and information using both physical contact and social network data offers a more realistic approach. However, acquiring data from both virtual and physical networks is challenging, as linking individual awareness and connections across these spaces is difficult. Real world data connecting virtual social networks to physical contact networks is scarce, so we opted for a representative dataset: the face-to-face contact network from the "Infectious Disease: Keep Away" exhibition held at the Science Gallery in Dublin in 2009.[40] This dataset includes $N = 410$ nodes and 17298 time-varying edges representing the interactions lasting at least 20 seconds. We use this dataset as the disease layer and as a basis to construct the high-order network for the information layer.

For the construction of the information layer, interactions in the face-to-face contact network are measured in 20-s intervals. We first aggregate the real data using a time window of $\Delta t = 5$ min and compute all the cliques that appear. Since our study is limited to cases involving $D = 2$, we need to generate a simplicial complex consisting of 1- and 2-simplices. Therefore, we consider all 2- and 3-cliques and weigh them based on their frequency. Note that while higher-dimensional cliques are not included in the final simplicial complex, their sub-cliques with a maximum size of 3 are considered in the count. We retain 80% of the most frequently occurring simplicial complexes. The constructed information layer network has N nodes in total. Additionally, the first-order average degree is $\langle k_{|} \rangle = 13.45$, and the second-order average degree is $\langle k_{\Delta} \rangle = 6.75$.

To construct the disease layer and characterize individual activity and attractiveness, we evaluate the activity a_i of node i as the percentage of active connections per unit time. It is de-

fined as $a_i = e_{i,\text{out}}/\sum_j^N e_{j,\text{out}}$, where $e_{i,\text{out}}$ represents the total active intensity of node i over the entire period. Similarly, attractiveness b_i is the proportion of passive contacts per unit time, calculated as $b_i = e_{i,\text{in}}/\sum_j^N e_{j,\text{in}}$, where $e_{i,\text{in}}$ represents the total passive intensity of node i over the same period.

We analyze the distributions of activity and attractiveness in the face-to-face contact network data, as shown in Fig. 11. Real-world networks typically exhibit truncated distributions for both activity and attractiveness ($F(a)$ and $F(b)$), which we fit using a truncated power-law distribution.[41] The fitting results reveal that both activity and attractiveness distributions show relatively low heterogeneity. Figure 11 demonstrates that the distribution of node activity and attractiveness aligns well with a truncated power-law distribution. This analysis suggests that the real-world dataset accurately reflects the activity characteristics of nodes, making the face-to-face contact network time-series suitable for studying the impact of information–epidemic coupling spread in real scenarios.

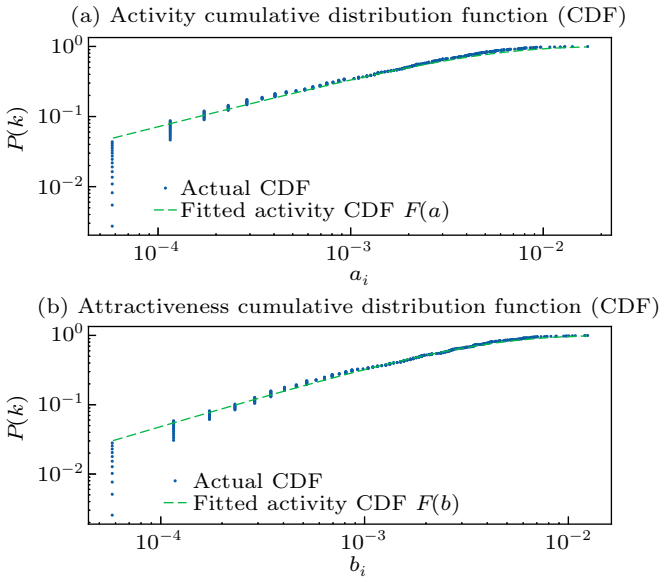


Fig. 11. Activity and attractiveness distributions of the face-to-face contact network. The blue solid circles represent the real data, and the red curve indicates the fitting result of the truncated power-law distribution $F(x) = cx^{-d}\,\mathrm{e}^{-hx}$. (a) Fitting result of the activity distribution $F(a)$, $c = 0.4126$, $d = 0.3015$, $h = 202$. (b) Attractiveness distribution $F(b)$, $c = 0.4256$, $d = 0.1254$, $h = 301$.

Finally, we examine the effects of individual behavioral responses in the real-world network. In Fig. 12(a), we find that as the self-protection factor ω decreases, the infection size ρ^{I} increases. The experimental results indicate that adopting self-protection measures can effectively suppress the epidemic spreading, which is consistent with the simulation results in the synthetic networks from Section 4. In Fig. 12(b), as the self-isolation factor η decreases, the infection size also ρ^{I} increases. The experimental results show that self-isolation measures similarly suppress the epidemic spread, corroborating the findings from the synthetic network simulations in Section 4 and demonstrating the effectiveness of our model in real-world networks.

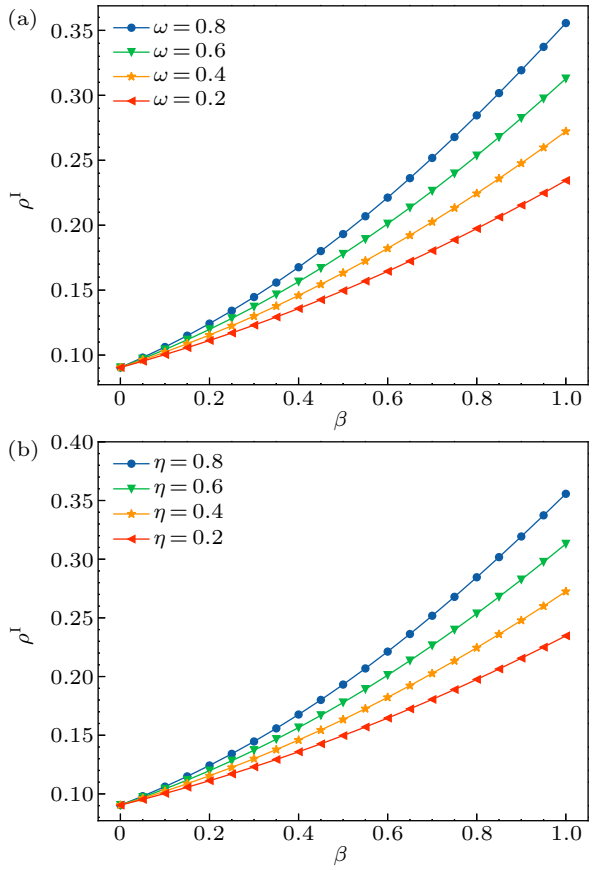


Fig. 12. The impact of (a) self-protection factor ω and (b) self-isolation factor η on epidemic spread in the face-to-face contact network.

6. Conclusion and perspectives

In situations with limited treatment options and scarce medical resources, individuals obtain information about epidemics through social behavior and adopt certain behavioral responses to prevent being infected, which helps in controlling the spread of the disease. Therefore, this paper considers factors such as message fatigue, higher-order interactions, and individual behavioral responses to epidemics. Under a two-layer network framework, a new UAF-SIS model is proposed to characterize the information–epidemic coupling spreading. Specifically, the virtual information layer is composed of a 2-simplicial complex structure, where individuals not only exchange information through direct interactions but also through group interactions facilitated by higher-order structures. Additionally, during the information dissemination process, individuals often experience fatigue from excessive information, leading to decreased vigilance towards the epidemic.

On the disease layer, an activity-driven model with attractiveness is utilized to describe changes in individual activity and attractiveness, reflecting various behavioral responses to the epidemic. Using this approach, we use the MMCA on the proposed model in order to get the state transition equations of the entire spread system and derive the epidemic out-

break threshold analytically. Subsequently, we explore the effects of different parameters on epidemic spread and utilize MC method to assess the influence of individual behavioral responses on the topology of the disease layer network.

The experimental results indicate that higher-order structures, which describe group reinforcement effects, facilitate information diffusion, thereby suppressing the epidemic spread. Message fatigue partially inhibits the information dissemination process, promoting the development of the epidemic. Individual self-protection and self-isolation behaviors help delay the epidemic outbreak and are highly effective in controlling its spread. Self-protection behaviors increase the number of low-degree nodes and decrease the proportion of high-degree nodes, leading to a reduction in the average degree $\langle k \rangle$ of the disease layer. Both self-protection and self-isolation behaviors contribute to the clustering of susceptible nodes in the disease layer network. Finally, we apply the model to real-world networks to verify its reliability and applicability.

Our work provides valuable insights for epidemic prevention efforts and offers useful recommendations for governments and social groups to develop effective measures for managing public health emergencies. When disseminating epidemic-related information, it is crucial to consider individuals' sensitivity to information to prevent fatigue, which could otherwise exacerbate the epidemic's spread. Future work will focus on the dynamics of information–epidemic coupling spreading, recognizing that individual behavioral responses are not static but adapt based on the surrounding infection environment. Additionally, while we have addressed some fundamental real-world features (e.g., contact heterogeneity, individual activity, and attractiveness, behavioral changes), other important aspects such as population age structure and preferential contacts remain unexplored.

Program availability

The source code is openly available in Science Data Bank at https://doi.org/10.57760/sciencedb.17567.

Acknowledgments

Project supported by the National Natural Science Foundation of China (Grant Nos. 72171136 and 72134004), Humanities and Social Science Research Project, Ministry of Education of China (Grant No. 21YJC630157), the Natural Science Foundation of Shandong Province (Grant No. ZR2022MG008), and Shandong Provincial Colleges and Universities Youth Innovation Technology of China (Grant No. 2022RW066).

References

[1] Jones K E, Patel N G, Levy M A, *et al.* 2008 *Nature* **451** 990
[2] Berche P 2022 *Presse Med.* **51** 104117
[3] Berche P 2022 *Presse Med.* **51** 104127
[4] Stone B M and Wang V 2023 *J. Affect. Disord. Rep.* **11** 100479
[5] Laing A G, Lorenc A, Del Molino, *et al.* 2020 *Nat. Med.* **26** 1623
[6] Newman M E J 2003 *SIAM Rev.* **45** 167
[7] Pastor-Satorras R and Vespignani A 2002 *Phys. Rev. E* **65** 036104
[8] Hu X, Chen J and Xia C 2024 *Chin. Phys. B* **33** 100202
[9] Yin Q, Wang Z and Xia C 2023 *Nonlinear Dyn.* **111** 14583
[10] Liu Y, Sanhedrai H, Dong G, *et al.* 2020 *Natl. Sci. Rev.* **8** nwaa229
[11] Funk S, Gilad E and Jansen V A A 2010 *J. Theor. Biol.* **264** 501
[12] Granell C, Gomez S and Arenas A 2013 *Phys. Rev. Lett.* **111** 128701
[13] Xie X and Huo L 2024 *Chaos, Solitons & Fractals* **181** 114586
[14] Sun Q, Wang Z, Zhao D, *et al.* 2022 *Chaos, Solitons & Fractals* **164** 112734
[15] Li L, Dong G, Zhu H, *et al.* 2024 *Appl. Math. Comput.* **472** 128617
[16] Wang Z, Xia C, Chen Z, *et al.* 2021 *IEEE Trans. Cybern.* **51** 1454
[17] Xia C, Wang Z, Zheng C, *et al.* 2019 *Inf. Sci.* **471** 185
[18] Peng P, Fan T and Lü L 2024 *Entropy* **26** 248
[19] Benson A R, Gleich D F and Leskovec J 2016 *Science* **353** 163
[20] Huang S, Chen J, Li M Y, *et al.* 2024 *Chin. Phys. B* **33** 030205
[21] Iacopini I, Petri G, Barrat A, *et al.* 2019 *Nat. Commun.* **10** 2485
[22] Wang H, Zhang H F, Zhu P C, *et al.* 2022 *Chaos* **32** 083110
[23] Zhang K, Hong X, Han Y, *et al.* 2024 *Chaos, Solitons & Fractals* **180** 114490
[24] Fan J, Zhao D, Xia C, *et al.* 2022 *Chaos* **32** 113115
[25] Wu B and Huo L 2024 *Chaos, Solitons & Fractals* **180** 114522
[26] Huo L A and Yu Y 2023 *Chaos, Solitons & Fractals* **169** 113229
[27] Pozzana I, Sun K and Perra N 2017 *Phys. Rev. E* **96** 042310
[28] Huo L A and Yu Y 2023 *Chin. Phys. B* **32** 108703
[29] Xu H, Xie W and Han D 2023 *Chaos* **33** 013110
[30] Xie X X, Huo L A, Dong Y F, *et al.* 2024 *Chin. Phys. B* **33** 038704
[31] Peng X L and Zhang Y D 2021 *Chin. Phys. B* **30** 058901
[32] Huo L, Liu B and Zhao X 2024 *Chin. Phys. B* **33** 128903
[33] Feng M, Liu L, Chen J, *et al.* 2024 *Chaos, Solitons & Fractals* **183** 114858
[34] Koh P, Chan L L and Tan E K 2020 *Arch. Med. Res.* **51** 716
[35] Liu H, Liu W, Yoganathan V, *et al.* 2021 *Technol. Forecast. Soc. Change.* **166** 120600
[36] Guo Y, Lu Z, Kuang H, *et al.* 2020 *Int. J. Inf. Manage.* **52** 102067
[37] Walker G R 2022 *AIDS Edu. Prev.* **34** 17
[38] Jhun B, Jo M and Kahng B 2019 *J. Stat. Mech.* **2019** 123207
[39] Alessandretti L, Sun K, Baronchelli A, *et al.* 2017 *Phys. Rev. E* **95** 052318
[40] Panzarasa P, Opsahl T and Carley K M 2009 *J. Am. Soc. Inf. Sci.* **60** 911
[41] Clauset A, Shalizi C R and Newman M E J 2009 *SIAM Rev.* **51** 661